

# Properties of the ENCE and other MAD-based calibration metrics

Pascal PERNOT <sup>1</sup>

*Institut de Chimie Physique, UMR8000 CNRS,  
Université Paris-Saclay, 91405 Orsay, France<sup>a)</sup>*

The Expected Normalized Calibration Error (ENCE) is a popular calibration statistic used in Machine Learning to assess the quality of prediction uncertainties for regression problems. Estimation of the ENCE is based on the binning of calibration data. In this short note, I illustrate an annoying property of the ENCE, i.e. its proportionality to the square root of the number of bins for well calibrated or nearly calibrated datasets. A similar behavior affects the calibration error based on the variance of  $z$ -scores (ZVE), and in both cases this property is a consequence of the use of a Mean Absolute Deviation (MAD) statistic to estimate calibration errors. Hence, the question arises of which number of bins to choose for a reliable estimation of calibration error statistics. A solution is proposed to infer ENCE and ZVE values that do not depend on the number of bins for datasets assumed to be calibrated, providing simultaneously a statistical calibration test. It is also shown that the ZVE is less sensitive than the ENCE to outstanding errors or uncertainties.

arXiv:2305.11905v1 [cs.LG] 17 May 2023

---

<sup>a)</sup>Electronic mail: [pascal.pernot@cnrs.fr](mailto:pascal.pernot@cnrs.fr)

## A. Definition of the ENCE

Various forms of Mean Absolute Deviation (MAD) statistics have been proposed to quantify the calibration error in Machine Learning (ML) classification<sup>1</sup> or regression problems<sup>2-4</sup> with Uncertainty Quantification (UQ). Among them, the Expected Normalized Calibration Error (ENCE) has been introduced recently by Levi *et al.*<sup>3,4</sup>, and used in several ML-UQ studies since<sup>5-9</sup>. I focus here on the ENCE, but its variants such as the Uncertainty Calibration Error (UCE or ECE) are also concerned.

Let us consider a set of prediction errors and uncertainties  $\{E_i, u_i\}_{i=1}^M$  arising from an ML-UQ regression problem. *Average* calibration can be tested by comparing the mean variance (MV) estimated from the uncertainties

$$\text{MV} = \frac{1}{M} \sum_{i=1}^M u_i^2 \quad (1)$$

to the variance of the errors, or in the hypothesis of unbiased errors ( $\bar{E} \simeq 0$ ), to the mean squared errors (MSE)

$$\text{MSE} = \frac{1}{M} \sum_{i=1}^M E_i^2 \quad (2)$$

Average calibration is known to be unreliable to characterize the properties of prediction uncertainties, notably because an average of overestimated and underestimated uncertainties might still provide a MV value in agreement with the MSE.<sup>10,11</sup> To avoid this, it was proposed to use *conditional* calibration, in which calibration is tested *locally* across the range of uncertainty values.<sup>3,4,12</sup> Conditional calibration with respect to uncertainty is also called *consistency*, to distinguish it from conditional calibration with respect to *input features*, which is called *adaptivity*.<sup>12,13</sup>

In order to test consistency, one procedure is to compare the MV to the MSE using *binned* data. For this, the dataset is ordered by increasing uncertainty values and split into  $N$  bins  $B_1, \dots, B_N$ , which is expected to reduce the possibility of compensation between over- and under-estimated uncertainties when the bin size is chosen small enough. The *local* calibration within bin  $i$  can be assessed by checking that the mean variance

$$\text{MV}_i = \frac{1}{|B_i|} \sum_{j \in B_i} u_j^2 \quad (3)$$

is equal to mean squared error

$$\text{MSE}_i = \frac{1}{|B_i|} \sum_{j \in B_i} E_j^2 \quad (4)$$

where  $|B_i|$  is the size of bin  $i$ .

*Reliability diagrams* are obtained by plotting  $\text{MSE}_i$  vs  $\text{MV}_i$  and by comparing the points to the identity line.<sup>3,4</sup> In order to quantify the amplitude of the differences between the error and uncertainty statistics, one estimates the ENCE metric, as the relative MAD between  $\text{MV}_i^{1/2}$  and  $\text{MSE}_i^{1/2}$

$$\text{ENCE} = \frac{1}{N} \sum_{i=1}^N \frac{|\text{MV}_i^{1/2} - \text{MSE}_i^{1/2}|}{\text{MV}_i^{1/2}} \quad (5)$$

The ENCE is typically reported as a percentage, and used to compare the performances of various calibration procedures on a given dataset.

## B. Impact of the binning scheme on ENCE estimation

One can observe in the literature a diversity of binning strategies to estimate the ENCE. Some authors use a small number of bins (typically 10-15)<sup>2,4,7,14</sup>, whereas other prefer much larger numbers<sup>5</sup>. There is also a choice between equal-size bins and equal-width bins, but for the present study I focus only on the former strategy.

Several considerations can help to define a proper number of bins. The use of a large number of bins seems more in agreement with the approach of conditional calibration, but smaller numbers of bins can be expected to provide more accurate statistics. It is indeed important that the bin size is kept large enough to preserve testing power when the bins are used to estimate test statistics<sup>10</sup>. For equal-size bins, the distribution of binned values is transformed to a uniform distribution, and entropy-based arguments for histograms provide the optimal number of bins as the square root of the sample size ( $N = M^{1/2}$ ).<sup>15</sup> This tends to favor rather large bin numbers for datasets with more than 1000 points.

As there is presently no consensus on the optimal binning strategy for the estimation of calibration errors, it is interesting to check how the choice of  $N$  influences ENCE values. In this perspective, let us first consider a slightly simplified problem to illustrate the estimation issues (a fully analytical example loosely related to the ENCE is also presented in Appendix 1). Assuming an homoscedastic dataset ( $u_i = u = c^{te}$ ), one can write

$$\text{ENCE} = \frac{1}{Nu} \sum_{i=1}^N |\text{MSE}_i^{1/2} - u| \quad (6)$$

For *normally* distributed errors ( $E_i \sim N(0, 1)$ ),  $\text{MSE}_i^{1/2}$  has a *chi distribution* with  $k$  degrees of freedom,  $\chi_k$ , where  $k$  is the size of a bin ( $k = \lfloor M/N \rfloor$ ). Due to the absolute value, the ENCE is thus based on the sum of shifted-folded  $\chi_k$  distributions, the properties of which have to be studied by simulation.

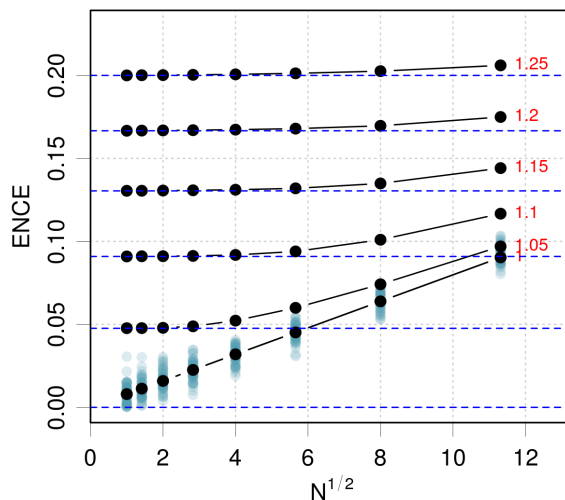


Figure 1. Dependence of the ENCE on the square root of the number of bins  $N^{1/2}$  for several miscalibration factors (red numbers). The dataset size is  $M = 5000$ . For each bin size  $k = M/N$ , the ENCE is estimated by Monte Carlo:  $N$  samples  $X$  of  $10^5$  points of a  $\chi_k$  variable are drawn; for each bin the sample mean of  $|X - u|/u$  is estimated; finally the ENCE is obtained by averaging over the bins. The blue dots represent 50 realizations of the estimation of ENCE from random  $E \sim N(0, 1)$  datasets analyzed by the `ErrViewLib::plotRelDiag` function.

Fig. 1 reports the dependence of the ENCE for a well calibrated dataset ( $u = 1$ ) and several levels of miscalibration, with  $u$  varying between 1.05 and 1.25. For the calibrated dataset ( $u = 1$ ) the ENCE estimated using the  $\chi_k$  distribution approach is proportional to  $N^{1/2}$ . To validate this result, a Monte Carlo simulation of ENCE values from random samples of  $E$  was performed and plotted as blue dots. The curve using the  $\chi_k$  distributions represents perfectly the average location of these points for each value of  $N$ , and as it is much less computer intensive, it was used for the other values of  $u$ . For uncalibrated datasets ( $u \neq 1$ ), one observes a transient behavior between a constant value (giving the correct relative error) for small values of  $N$  and a linear dependence with  $N^{1/2}$  as  $N$  increases. The constant part becomes predominant as  $u$  increases.

This transient behavior of the ENCE is due to the properties of the MAD, which measures a bias when all deviations  $\text{MSE}_i^{1/2} - u$  are of the same sign (the ENCE is independent of  $N$ ) and a dispersion when  $\text{MSE}_i^{1/2} \simeq u$  (the ENCE depends on the uncertainty of the binned statistic, see Appendix 1).<sup>16</sup>

The ENCE seems thus well adapted to characterize a lack of calibration, and using small numbers of bins as often done in the literature seems to provide a reliable estimation of the

relative calibration error. However, one is facing a problem when testing a calibrated dataset, for which any reasonable value of  $N$  gives a non-zero and different estimation of the ENCE. In this case, the ENCE is dominated by the statistical fluctuations of the binned values. For our model example, using  $N = 36$  bins would give a 5% ENCE. How does this inform us on the calibration of this dataset ?

One might be tempted to use the  $N^{1/2}$  law as a baseline to test calibration, but the proportionality constant is sensitive to the errors and uncertainties distribution, and therefore dataset-dependent (see Table I). A better solution could be to perform a linear regression of ENCE values obtained for several values of  $N$  versus  $N^{1/2}$  and compare the intercept to 0 (the confidence interval for the intercept of a perfectly calibrated dataset should include 0). This method is tested below.

### C. Definition of the Z-Variance Error (ZVE)

An alternative way to test calibration<sup>11</sup> is to check that the variance of  $z$ -scores is equal to 1

$$\text{Var}(Z = E/u) = 1 \quad (7)$$

which extends directly to individual bins

$$v_i = \text{Var}\left(\{Z_j = E_j/u_j\}_{j \in B_i}\right) = 1 \quad (8)$$

as used in the Local Z-Variance (LZV) analysis.<sup>11</sup> This approach is preferable to the MV/MSE approach as it accounts explicitly for the pairing of errors and uncertainties and is less susceptible to fortuitous compensations.

Following the same ideas as for the ENCE, I define a Z-Variance Error (ZVE) as the mean deviation from 1 of the binned  $v_i$  statistics

$$\text{ZVE} = \exp\left(\frac{1}{N} \sum_{i=1}^N |\ln v_i|\right) \quad (9)$$

accounting for the fact that the  $v_i$  are dimensionless scale statistics. The ZVE is therefore also a MAD-based statistic, but it should provide a more reliable assessment of local calibration, notably for schemes with large bins. It is compared to the ENCE in the following section.

### D. Application to ML-UQ datasets

The observations made above for a toy model are now tested on three recent ML-UQ datasets, for both the ENCE and ZVE statistics. In all cases, the number  $N$  of equal-size bins is varied between 1 and a maximum value chosen to avoid bins with less than 30 points.

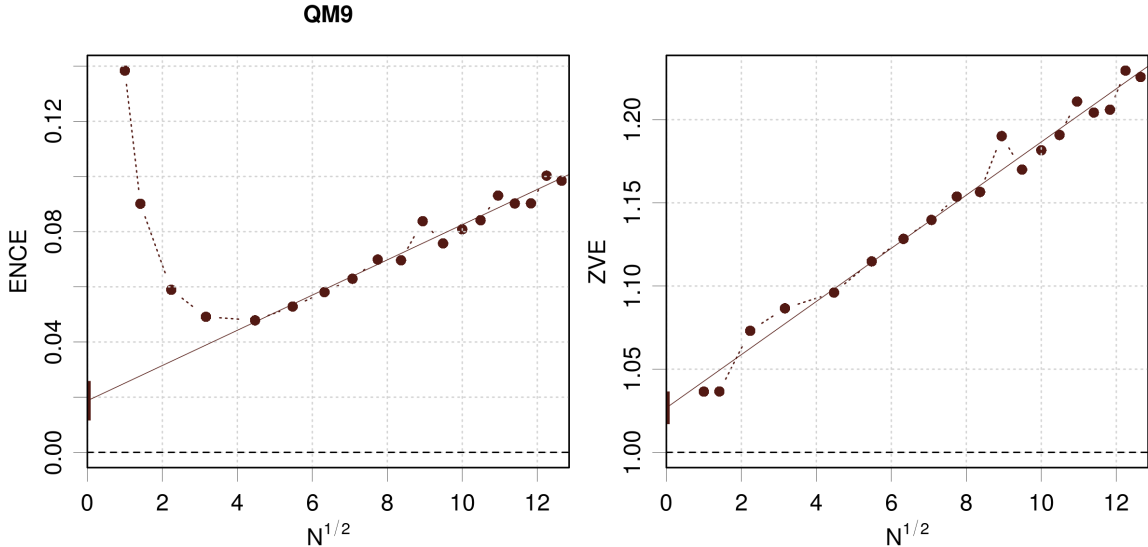


Figure 2. Dependence of the ENCE and ZVE on the square root of the number for bins  $N^{1/2}$  for the BUS2022 QM9 dataset. The linear fits (solid lines) are based on the points with  $N^{1/2} > 4$  for the ENCE and all points for the ZVE. The vertical line segment at the origin represents the 95% confidence interval on the fit intercept.

### 1. Case BUS2022

This dataset has been presented in Busk *et al.*<sup>7</sup> and reused in a previous study<sup>12</sup>. The QM9 validation dataset consists of  $M = 13\,885$  predicted atomization energies ( $V$ ), uncertainties ( $u_V$ ), and reference values ( $R$ ). In absence of uncertainty on the reference values, these data are transformed to  $E = R - V$  and  $u = u_V$ .

The estimation of the ENCE as a function of the number of bins is presented in Fig. 2. The curve presents a rise at small values of  $N$  which was not observed for the toy problem. In fact, this dataset presents several outstanding errors at large uncertainties, which produce a large ENCE contribution into a single bin. The impact of this outstanding bin statistic gets averaged out as the number of bins increases. Above about 20 bins, the ENCE rejoins a linear trend with  $N^{1/2}$ . Busk *et al.*<sup>7</sup> report a value of  $\sim 5\%$  for 15 bins, consistent with our estimation for  $N^{1/2} = 4$ . The linear fit of the values above  $N^{1/2} = 4$  provides an intercept value of  $\sim 0.019(3)$  (Table I), i.e. a  $\sim 2\%$  residual relative calibration error which is significantly different from 0.

In contrast, the ZVE statistic is not notably impaired by the outliers and displays a consistent linear trend with  $N^{1/2}$  over the whole range. The linear fit using all points provides an intercept of  $\sim 1.027(4)$  (Table I), i.e. a  $\sim 2.7\%$  relative error on variance calibration, significantly different from 0.

Statistic Set		Intercept	Slope
ENCE	QM9	0.019(3)	0.0064(3)
	Diffusion	0.06(1)	0.013(2)
	Perovskite	0.071(6)	0.0149(8)
ZVE	QM9	1.027(4)	0.0160(5)
	Diffusion	1.11(4)	0.039(6)
	Perovskite	1.11(2)	0.053(2)

Table I. Coefficients of the linear fits with respect to  $N^{1/2}$  for the ENCE and ZPE statistics of the three studied datasets.

Both calibration statistics therefore lead us to conclude that the dataset has small residual calibration errors, but at a level that is even smaller than the 5% that the original authors considered as a “low ENCE”<sup>7</sup>.

## 2. Case PAL2022

The data have been gathered from the supplementary information of a recent article by Palmer *et al.*<sup>14</sup> and previously reanalyzed<sup>12</sup>. I retain here two sets of errors and uncertainties *before* and *after* calibration by a bootstrapping method and resulting from the application of a random forest regression to two materials datasets (Diffusion,  $M = 2040$  and Perovskites,  $M = 3836$ ). The reader is referred to the original article for more details on the methods and datasets.

The dependence of the ENCE and ZVE with  $N^{1/2}$  are presented in Fig. 3. Let us first consider the *uncalibrated* datasets (black dots). Although the dependence on  $N^{1/2}$  is sensible, there is no doubt that the ENCE is about 30% for the Diffusion data. Considering the shape of the curve with a fall-off below  $N^{1/2} = 3$ , the ENCE value is more difficult to appreciate for the Perovskite data, but lies probably around 25%. The ZVE curves for both datasets present a transition around 4-6 from a more or less constant curve to a linear increase with  $N^{1/2}$ . For these data, using  $N = 15$  seems to be a reasonable choice as it falls within the more or less constant part of the curve.

The curves for the calibrated data (red triangles) also present deviations from linearity below  $N^{1/2} = 4$  for Diffusion and  $N^{1/2} = 2$  for Perovskite. The corresponding values are excluded from the linear fit, which leaves only 6 points for the Diffusion dataset and 13 points for the Perovskite. Nevertheless, the values and confidence intervals of the intercepts (Table I) lead to conclude to significant residual calibration errors for both datasets, between 5 and 10% for the

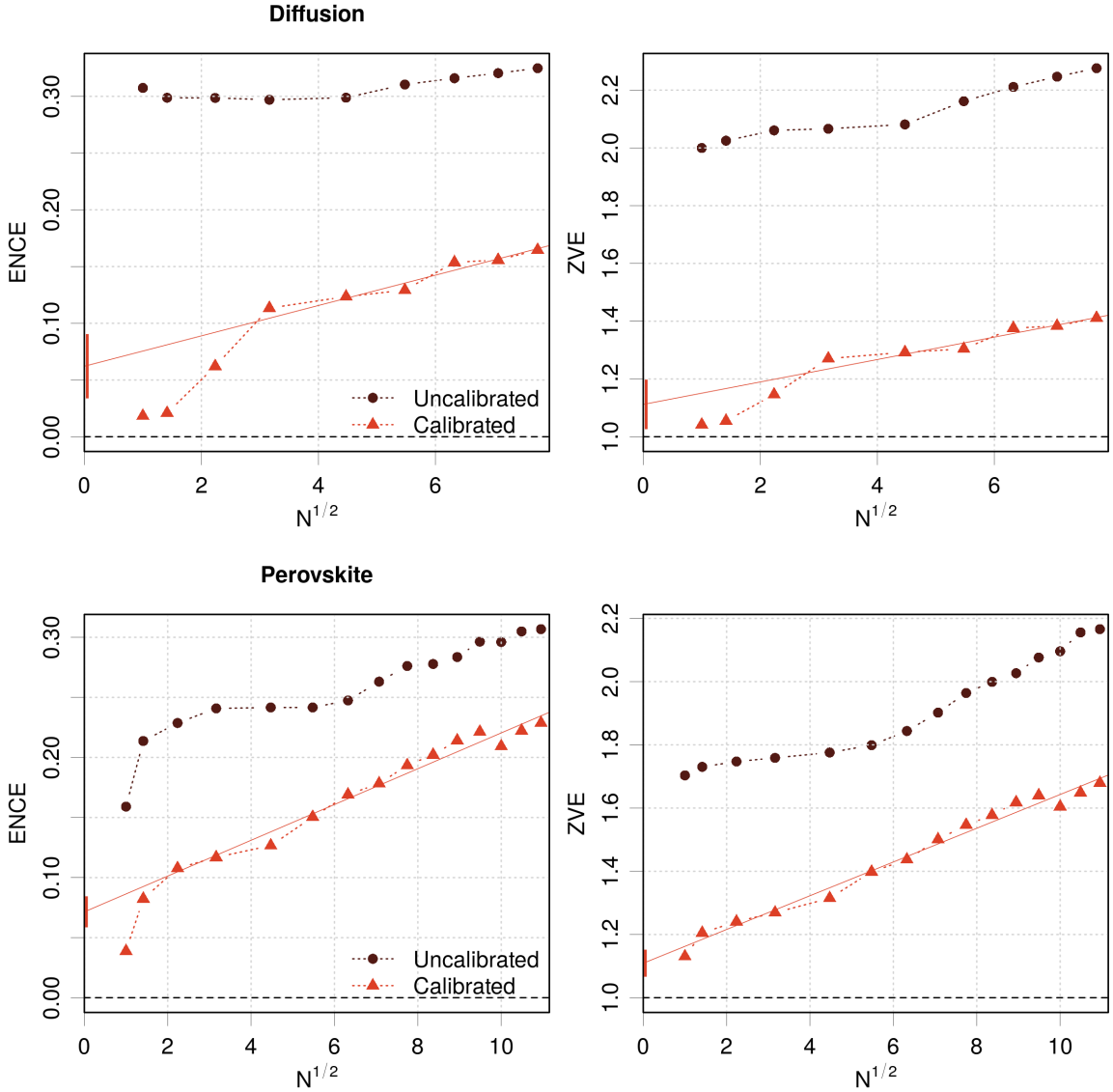


Figure 3. Dependence of the ENCE and ZVE on the square root of the number for bins  $N^{1/2}$  for the PAL2022 Diffusion and Perovskite dataset. The linear fits of the calibrated data (dashed lines) are based on the points with  $N^{1/2} > 4$  for Diffusion and  $N^{1/2} > 2$  for Perovskite. The vertical line segment at the origin represents the 95% confidence interval on the linear fit intercept.

ENCE and about 10% for the ZVE.

## E. Conclusions

I have shown through synthetic and ML-UQ datasets that usual calibration statistics, such as the ENCE and its alternative ZVE, are strongly sensitive to the choice of the number of bins  $N$  for calibrated or nearly calibrated datasets. Both statistics are globally linear in  $N^{1/2}$ , a behavior that can be traced to the use of the MAD statistic, which is a location estimator for



sets with large bias and a dispersion estimator for unbiased sets. Not treated in this study, metrics based on maximal deviations are also expected to be dependent on the binning scheme, in a more trivial way.

A consequence is that comparisons of MAD-based calibration statistics should always be done on the basis of identical binning schemes. Another important issue is that interpretation of these calibration statistics might be problematic when comparing uncalibrated and calibrated datasets, as they do not convey the extent of residual calibration errors for the latter. I have shown that the intercept from a linear fit with respect to  $N^{1/2}$  of a calibration statistic for a series of bin numbers can provide a more reliable estimation of the calibration error and can also be used as a calibration test.

It appears also that the ZVE is less sensitive than the ENCE to outstanding values in the datasets, which might make it a more suitable calibration error statistic.

## Acknowledgments

I warmly thank J. Busk for providing me the data of the BUS2022 case.

## Author Declarations: Conflict of Interest

The author has no conflicts to disclose.

## Code and data availability

The code and data to reproduce the results of this article are available at [https://github.com/ppernot/2023\\_ENCE/releases/tag/v0.0](https://github.com/ppernot/2023_ENCE/releases/tag/v0.0) and at Zenodo (<https://doi.org/10.5281/zenodo.7943886>). The R,<sup>17</sup> `ErrViewLib` package implements the `plotRelDiag` and `plotLZV` functions used in the present study to estimate the ENCE and ZVE, respectively, under version `ErrViewLib-v1.7.1` (<https://github.com/ppernot/ErrViewLib/releases/tag/v1.7.1>), also available at Zenodo (<https://doi.org/10.5281/zenodo.7943906>).

## REFERENCES

- <sup>1</sup>C. Guo, G. Pleiss, Y. Sun, and K. Q. Weinberger. [On Calibration of Modern Neural Networks](#). In *International Conference on Machine Learning*, pages 1321–1330. 2017. URL: <https://proceedings.mlr.press/v70/guo17a.html>.

- <sup>2</sup>M.-H. Laves, S. Ihler, J. F. Fast, L. A. Kahrs, and T. Ortmaier. [Well-calibrated regression uncertainty in medical imaging with deep learning](#). In T. Arbel, I. Ben Ayed, M. de Bruijne, M. Descoteaux, H. Lombaert, and C. Pal, editors, *Proceedings of the Third Conference on Medical Imaging with Deep Learning*, volume 121 of *Proceedings of Machine Learning Research*, pages 393–412. PMLR, 06–08 Jul 2020. URL: <https://proceedings.mlr.press/v121/laves20a.html>.
- <sup>3</sup>D. Levi, L. Gispan, N. Giladi, and E. Fetaya. [Evaluating and Calibrating Uncertainty Prediction in Regression Tasks](#). *arXiv:1905.11659*, 2020. URL: <http://arxiv.org/abs/1905.11659>.
- <sup>4</sup>D. Levi, L. Gispan, N. Giladi, and E. Fetaya. [Evaluating and Calibrating Uncertainty Prediction in Regression Tasks](#). *Sensors*, 22(15):5540, 2022.
- <sup>5</sup>G. Scalia, C. A. Grambow, B. Pernici, Y.-P. Li, and W. H. Green. [Evaluating scalable uncertainty estimation methods for deep learning-based molecular property prediction](#). *J. Chem. Inf. Model.*, 60:2697–2717, 2020.
- <sup>6</sup>D. Wang, J. Yu, L. Chen, X. Li, H. Jiang, K. Chen, M. Zheng, and X. Luo. [A hybrid framework for improving uncertainty quantification in deep learning-based QSAR regression modeling](#). *J. Cheminf.*, 13, 2021.
- <sup>7</sup>J. Busk, P. B. Jørgensen, A. Bhowmik, M. N. Schmidt, O. Winther, and T. Vegge. [Calibrated uncertainty for molecular property prediction using ensembles of message passing neural networks](#). *Mach. Learn.: Sci. Technol.*, 3:015012, 2022.
- <sup>8</sup>L. I. Vazquez-Salazar, E. D. Boittier, and M. Meuwly. [Uncertainty quantification for predictions of atomistic neural networks](#). *arXiv:2207.06916*, July 2022.
- <sup>9</sup>L. Frenkel and J. Goldberger. [Calibration of a regression network based on the predictive variance with applications to medical images](#). 2023. URL: [https://www.eng.biu.ac.il/goldbej/files/2023/04/LIor\\_ISBI\\_2023.pdf](https://www.eng.biu.ac.il/goldbej/files/2023/04/LIor_ISBI_2023.pdf).
- <sup>10</sup>P. Pernot. [The long road to calibrated prediction uncertainty in computational chemistry](#). *J. Chem. Phys.*, 156:114109, 2022.
- <sup>11</sup>P. Pernot. [Prediction uncertainty validation for computational chemists](#). *J. Chem. Phys.*, 157:144103, 2022.
- <sup>12</sup>P. Pernot. [Validation of uncertainty quantification metrics: a primer based on the consistency and adaptivity concepts](#). *arXiv:2303.07170*, 2023. [arXiv:2303.07170](https://arxiv.org/abs/2303.07170).
- <sup>13</sup>A. N. Angelopoulos and S. Bates. [A Gentle Introduction to Conformal Prediction and Distribution-Free Uncertainty Quantification](#). *arXiv:2107.07511*, July 2021.

- <sup>14</sup>G. Palmer, S. Du, A. Politowicz, J. P. Emory, X. Yang, A. Gautam, G. Gupta, Z. Li, R. Jacobs, and D. Morgan. [Calibration after bootstrap for accurate uncertainty quantification in regression models](#). *npj Comput. Mater.*, 8:1–9, 2022.
- <sup>15</sup>S. Watts and L. Crow. [The Shannon Entropy of a Histogram](#). *arXiv:2210.02848*, October 2022.
- <sup>16</sup>P. Pernot and A. Savin. [Probabilistic performance estimators for computational chemistry methods: the empirical cumulative distribution function of absolute errors](#). *J. Chem. Phys.*, 148:241707, 2018.
- <sup>17</sup>R Core Team. *R: A Language and Environment for Statistical Computing*. R Foundation for Statistical Computing, Vienna, Austria, 2019. URL: <http://www.R-project.org/>.

## APPENDIX

### 1. MAD of binned statistics

Let us consider a set of  $M$  draws from a zero-centered (unbiased) normal distribution  $X \sim N(0, u_X)$ . These data are binned into  $N$  equal-size bins of size  $k$  (assuming for convenience that  $M$  is always divisible by  $N$ ). The average of  $X$  is estimated within each bin

$$\mu_j = \frac{1}{k} \sum_{i \in B_j} X_i \quad (10)$$

and the uncertainty on the mean is

$$u_j \simeq \frac{u_X}{\sqrt{k}} = u_X \sqrt{\frac{N}{M}} \quad (11)$$

from which one estimates the MAD of  $\mu_j$

$$m = \frac{1}{N} \sum_{j=1}^N |\mu_j| \quad (12)$$

As  $\mu_j$  has a zero-centered normal distribution,  $|\mu_i|$  has a half-normal distribution with mean  $\overline{\mu_j} = u_j \sqrt{2/\pi}$ , making the link of the MAD with a dispersion statistic. Finally, the mean value for the MAD is

$$m = u_X \sqrt{\frac{2}{\pi M}} \sqrt{N} \quad (13)$$

Therefore,  $m$  is proportional to  $N^{1/2}$ , showing the direct impact of the binning strategy on the value of  $m$ .